DE GRUYTER

Chemical Papers
DOI: 10.1515/chempap-2015-0228

ORIGINAL PAPER

Synthesis and properties of novel reusable nano-ordered KIT-5-*N*-sulfamic acid as a heterogeneous catalyst for solvent-free synthesis of 2,4,5-triaryl-1*H*-imidazoles

[a,b]Razieh Mirsafaei, [c]Majid M. Heravi*, [d]Shervin Ahmadi, [c]Tayebeh Hosseinnejad

[a]*Department of Chemistry, Yazd Branch, Islamic Azad University, Yazd, 89168-71967, Iran*

[b]*Young Researcher Club, Shahreza Branch, Islamic Azad University, Shahreza, Isfahan, 63731-93719, Iran*

[c]*Department of Chemistry, Alzahra University, Vanak, 19938-93973, Tehran, Iran*

[d]*Iran Polymer and Petrochemical Institute, Tehran, 14977-13115, Iran*

Received 16 June 2015; Revised 5 September 2015; Accepted 16 September 2015

A novel silica-bonded propyl-*N*-sulfamic acid nanocatalyst ($NHSO_3H$-KIT-5) supported on modified silica mesopore KIT-5 as an organic–inorganic hybrid with high specific surface area was successfully prepared. The 3-aminopropyltriethoxysilane (APTES) on KIT-5 was reacted with chlorosulfonic acid and accurately characterized by the FT-IR, XRD, SEM, EDAXS, and TGA techniques. This heterogeneous and recyclable catalyst catalyzed one pot, multicomponent condensation of benzil, aromatic aldehydes, and ammonium acetate in the presences of 0.05 g of nanocatalyst under solvent-free conditions to afford triaryl-imidazoles in excellent yields. This catalyst showed high catalytic activity under green conditions. This reaction was performed under open air conditions and required no special reaction conditions or chromatographic separation for purification.

Keywords: KIT-5 nanosilica, heterogeneous catalysis, solvent-free conditions, organic–inorganic hybrids, density functional theory, quantum theory of atoms in molecules

Introduction

Multisubstituted imidazoles are an important heterocyclic nucleus due to their well-known biological properties and play vital roles in biochemical processes. The imidazole moiety is present in several prescribed drugs, such as metronidazole, dacarbazine, cimetidine, thyroliberin, flumazenil, methimazole, and etomidate (Blotny, 2006; Hamon et al., 2009; Silva et al., 2001, 2007).

A literature survey revealed an enormous number of methods for the synthesis of imidazole derivatives via one pot three-component condensation of appropriate aromatic aldehydes, ammonium acetate, and benzil/benzoin in the presence of different catalysts. Our group has been engaged in the catalyzed synthesis of imidazoles using ionic liquids (Siddiqui et al., 2005), silica sulfuric acid (Shaabani & Rahmati, 2006), acetic acid (Sarshar et al., 1996), potassium aluminium sulfate (Mohammadi et al., 2008), sulfanilic acid (Mohammed et al., 2007), $NiCl_2 \cdot 6H_2O$ (Heravi et al., 2007a), H_3PO_4 (Wang et al., 2012), L-proline (Samai et al., 2009), zirconium(IV)-modified silica gel (Sharma & Sharma, 2011), Wells–Dawson heteropolyacid (Karimi et al., 2010), MCM-41-SO_3H (Mobil Composition of Matter No. 41) (Mahdavinia et al., 2012), $BF_3 \cdot SiO_2$ (Sadeghi et al., 2008), solid alumina (Li et al., 2012), $Zr(acac)_4$ (Khosropour, 2008), and I_2 (Mazaahir et al., 2007). These methods have their own advantages and drawbacks. Some of the

---

*Corresponding author, e-mail: mmh1331@yahoo.com

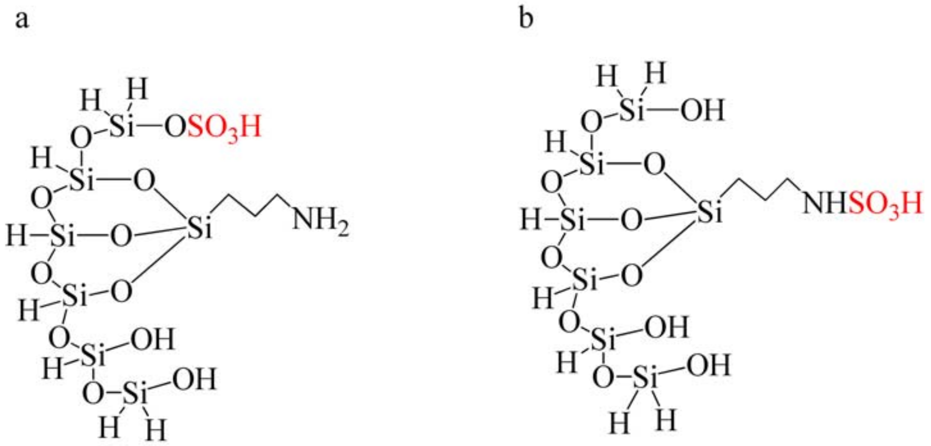

Fig. 1. Two effective structure models of supported solid acid aminated KIT-5 nanocatalyst denoted as O-SO_3H/KIT-5 (a) and N-SO_3H/KIT-5 (b).

drawbacks are low yields, long reaction times, and some requires the need of hazardous and hardly affordable catalysts with problematic recovery. Most of them are carried out in organic solvents and tedious work-up procedures and purification by expensive column chromatography were required. Thus, the synthesis and use of novel catalysts, especially nanocatalysts which may circumvent these problems is desired.

Nowadays, heterogeneous catalysis is an attractive and superior process in many areas of synthetic organic chemistry due to its unique properties such as the ease of separation and reusability (Guisnet et al., 1988; Tao et al., 2014). In heterogeneous catalysis, the quality and also the quantity of the surface area for the catalyst are important. Silica is a good choice as support for heterogeneous catalysis due to its maximum surface area. Mesoporous silica materials have attracted increasing interest in recent years. SBA-16 (Santa Barbara Amorphous-16), SBA-1, and KIT-5 (Korea Institute of Technology No. 5) are good examples of such porous materials (Bamoharram et al., 2007; Heravi et al., 2006a). The most common step toward surface area maximization is employing a support, a suitable material that the catalysts could be spread over (Suib, 2013). The three-dimensional pore architecture is usually the ideal support for this purpose.

Many types of *N*-sulfamic solid acid functionalized silica gels have been prepared and applied as an alternative to conventional sulfonic acid resins and homogeneous acids used as an efficient catalyst for different chemical transformations (Zhao et al., 2014; Khorami & Shaterian, 2014; Nouri Sefat et al., 2011). These catalysts have been applied to many acid-catalyzed reactions successfully, for example esterification (Schaubroeck et al., 2009, 2010; Silva et al., 2006), condensation of aldehydes with alcohol (Shvo & Goldman-Lev, 2002), Beckmann rearrangement (Martín & Garrone, 2003), and imidazole synthesis (Liu et al., 2008; Mannam & Sekar, 2008; Fan et al., 2010; Heravi et al., 2008a). Recently, in situ prepared copper nanoparticles on modified KIT-5 as an efficient recyclable catalyst and their application in click reactions in water have been reported (Mirsafaei et al., 2015).

Synthesis of heterogeneous catalysts and their applications in a variety of organic reactions in solvent-free condition is in the centre of our interest (Heravi & Sadjadi, 2009; Heravi et al., 2006a, 2006b, 2007b, 2007c, 2007d; Oskooie et al., 2006a); a review, entitled as “Current advances in the syntheses and biological potencies of tri- and tetra-substituted 1*H*-imidazoles” has also been published (Heravi et al., 2015). In continuation of our attempts to develop catalyzed synthetic ways (Heravi et al., 2000, 2007a, 2007d, 2008a, 2008b; Davoodnia et al., 2010; Oskooie et al., 2006b; Zeinali-Dastmalbaf et al., 2011; Moghaddas et al., 2012), in particular using nanocatalysts (Nemati et al., 2012; Heravi & Alishiri, 2012; Heravi et al., 2014, 2010, 2009a; Hashemi et al., 2014), and recent successful attempts to synthesize modified 3D-nanocage KIT-5 (Mirsafaei et al., 2015); in this paper, we wish to report the preparation of an *N*-sulfamic acid nanocatalyst supported on modified 3D-nanocage KIT-5. This catalyst has been prepared from commercially inexpensive commonly purchasable materials.

Theoretical

In the next step, comparative assessment of the chelating behavior of SO_3H group onto NH_2-KIT-5 was assessed by performing theoretical calculations using density functional theory (DFT) (Lee et al., 1988) and quantum theory of atoms in molecules (QTAIM) (Bader, 1990; Bader & Essén, 1984) approaches. Strictly speaking, two effective models for supported solid acid nanocatalyst (as illustrated in Fig. 1) were employed to comparatively analyze the preference of sulfur atom of SO_3H group in chelation with nitrogen or oxygen atoms onto NH_2-KIT-5

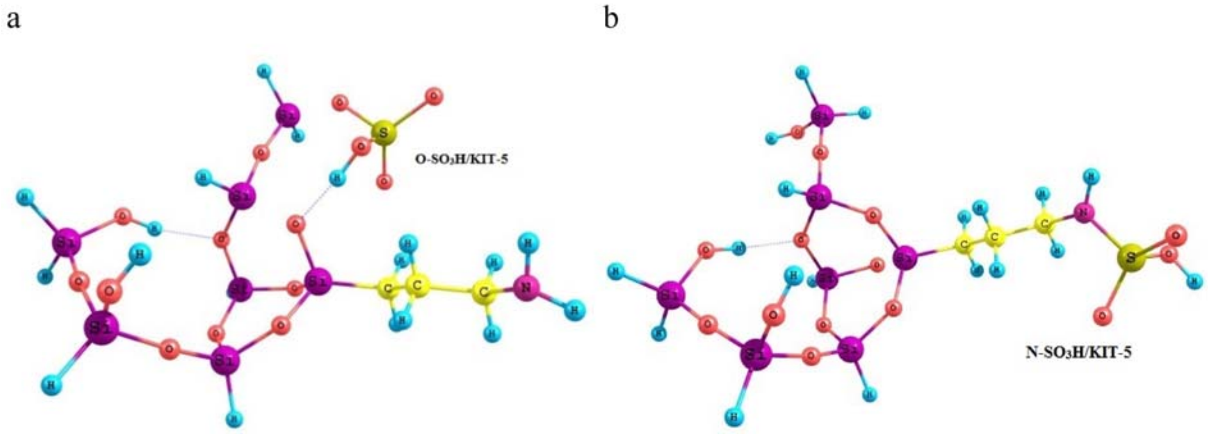

Fig. 2. The energy-minimized structure of O-SO_3H/KIT-5 (a) and N-SO_3H/KIT-5 (b) together with the calculated O—S and N—S bond orders obtained at M06/6-31G* level of theory.

Table 1. Mathematical properties of two selected N—S and O-S BCPs in N-SO_3H/KIT-5 and O-SO_3H/KIT-5; the properties were obtained by QTAIM analysis on the M06/6-311+G** calculated wave function of electron density (note that all calculated vaules are in atomic units system)

	ρ_b	$\nabla^2\rho_b$	G_b	V_b	H_b	$\lvert V_b\rvert/G_b$
N-SO_3H/KIT-5 N—S BCP	0.228	–0.571	0.120	–0.383	–0.263	3.191
O-SO_3H/KIT-5 O···H BCP	0.049	0.162	0.045	–0.050	–0.005	1.111

(N-SO_3H/KIT-5 or O-SO_3H/KIT-5). It should be noticed that, from the computational viewpoint, this model has a reliable comprise between accuracy and time saving efficiency of the computational procedure.

In this respect, the optimized structure of N-SO_3H/KIT-5 and O-SO_3H/KIT-5 was first calculated using DFT computations at M06/6-31G* level of theory. It should be stated that M06 functional has been introduced recently as a top performer among modern functionals, providing high performance and accuracy. Moreover, this functional was recommended for application in organometallic and non-organometallic thermochemistry, kinetic studies, and noncovalent interactions (Zhao & Truhlar, 2008). All DFT computations have been performed using GAMESS suite of programs (Schmidt et al., 1993). In Fig. 2, the theoretical optimized structures of N-SO_3H/KIT-5 and O-SO_3H/KIT-5 compounds are presented. Based on the structural features of N-SO_3H/KIT-5 and O-SO_3H/KIT-5 compounds (Fig. 2), it can be claimed that covalent bond formation between sulfonic acid and NH_2 group is more favorable than that of the OH group onto NH_2-KIT-5 while in O-SO_3H/KIT-5, O···H hydrogen bond is formed instead of O—S covalent bond.

In order to present a more concise interpretation of the chelating behavior of NH_2-KIT-5 with sulfur atom of chlorosulfonic acid, topological analysis of M06/6-311+G** calculated wave functions of electron density was performed. It is important to mention that the wave functions of electron density are correspond to M06/6-31G* optimized structures of N-SO_3H/KIT-5 and O-SO_3H/KIT-5. Thus, electronic energy density indicators were assessed at some key bond critical points (BCPs) using AIM2000 program package (Bader, 2000).

In Table 1, QTAIM calculated values of electron density, ρ_b, its Laplacian, $\nabla^2\rho_b$, electronic kinetic energy density, G_b, electronic potential energy density, V_b, total electronic energy density, H_b, and $\lvert V_b\rvert/G_b$ ratio are presented at some selected bond critical points (BCPs) for N-SO_3H/KIT-5 and O-SO_3H/KIT-5. It should be noticed that the values of electron density and the sign of electron density Laplacian at BCPs usually correlate with the strength of the covalent bond between two atoms. Furthermore, a good reliable indicator for classifying interatomic interactions as shared, closed-shell, and also hydrogen bonds is the total electronic energy density defined as $H_b = G_b + V_b$ at BCPs. In the closed-shell interactions, H_b has a positive value, for shared interactions it is negative, and for hydrogen bonds, H_b vanishes where $G_b \approx \lvert V_b\rvert$. Based on the QTAIM calculated data in Table 1, it can be concluded that N—S covalent bond in N-SO_3H/KIT-5 is formed with the corresponded negative values of $\nabla^2\rho_b$ and H_b correlating with the stabilization of the shared electrons on N—S BCP while the negative value of V_b together with the

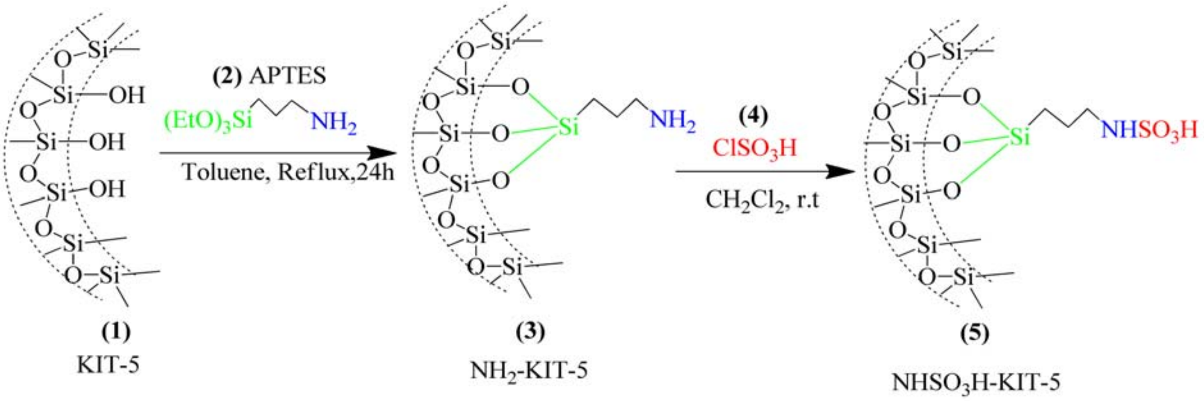

Fig. 3. Preparation of *N*-sulfamic solid acid nanocatalyst supported on KIT-5 ($NHSO_3H$-KIT-5).

Table 2. Physicochemical properties of mesoporous silica KIT-5 sample

BET surface area	Pore volume, V_p	BJH pore diameter	d_{111}	Unit cell parameter, a_0
$m^2\ g^{-1}$	$cm^3\ g^{-1}$	nm	nm	nm
1090	0.71	2.62	10.38	17.98

low value of H_b on O···H BCP confirm the hydrogen bond character of O···H in O-SO_3H/KIT-5. The calculated electronic results lead to the fact that the sulfur atom is chelated with nitrogen atom onto NH_2-KIT-5 rather than onto the oxygen atom, which confirms the experimental observations concerning immobilization of SO_3H inside the mesopores of KIT-5 and preparation of acid catalysts on N-SO_3H/KIT-5.

Experimental

All reagents were purchased from Fluka (Germany), Merck (Germany), and Sigma–Aldrich (USA) companies and used without further purification. All products were identified by comparison of their spectral and physical data with those of authentic samples reported. General properties of 3D highly interconnected nanocage-like mesoporous silica of the KIT-5 type, illustrated in Table 2 (Mirsafaei et al., 2015).

Catalyst preparation

Aminated KIT-5 was synthesized according to our previously reported procedure (Mirsafaei et al., 2015). A suspension of calcined KIT-5 (1.00 g) (1) and APTES (1.00 g) (2) in toluene (20 mL) as a solvent was refluxed with continuous stirring under N_2 atmosphere for 24 h. The unreacted APTES was removed by Soxhlet extraction using dry dichloromethane for 20 h and dried at 60 ℃. The sample was denoted as NH_2-KIT-5 (3) (Mirsafaei et al., 2015). To this residue in dry CH_2Cl_2 (3 mL) in a round-bottomed flask in an ice bath and under reduced pressure, chlorosulfonic acid (4) (0.6 mL as a > 97 % standard solution) was added dropwise in 5 min and stirred for 2 h. After this addition was complete, the mixture was stirred for another 2 h at room temperature in order to complete the elimination of HCl vapors. The mixture was filtered, washed with ethanol (2 × 25 mL), and dried at room temperature. The sample was denoted as *N*-sulfamic acid supported NH_2-KIT-5 ($NHSO_3H$-KIT-5) (5) in form of yellow powder (Fig. 3).

IR spectrum of NH_2-KIT-5, ν_{max}/cm^{-1}: 3643.47 (br), 2934.29 (m), 1582.18 (s), 1482.33 (m), 1081.39–1044.92 (s), 801.07 (s), 694.31 (w), 454.97 (s).

IR spectrum of $NHSO_3H$-KIT-5, ν_{max}/cm^{-1}: 3638.01 (br), 3081.63 (br), 1169.36 (s), 1059.17 (s), 796.21 (w), 587.01 (s), 461.08 (s).

Synthesis of 2,4,5-triphenyl imidazoles

In a round bottomed flask, a mixture of benzil (1.0 mmol), appropriate aldehyde (1.0 mmol), ammonium acetate (2.0 mmol), and $NHSO_3H$-KIT-5 as a catalyst (0.05 g) was stirred at room temperature. Then, the reaction mixture was heated to 120 ℃ in an oil bath under solvent-free conditions (Fig. 4) for the required period of time and monitored by TLC (ethyl acetate : hexane; φ_r = 7 : 3) as indicated in Table 3. In order to recover the catalyst, the residue was stirred in acetone (10 mL) for 10 min, washed further with acetone, dried under reduced pressured at 70 ℃ for 3 h, and stored for another consecutive reaction run. The filtrate was then evaporated to dryness under reduced pressure to afford the corresponding imidazole as pure crystals which were washed with 10 mL of ether. All imidazoles were known and their physical data were compared with those of authentic

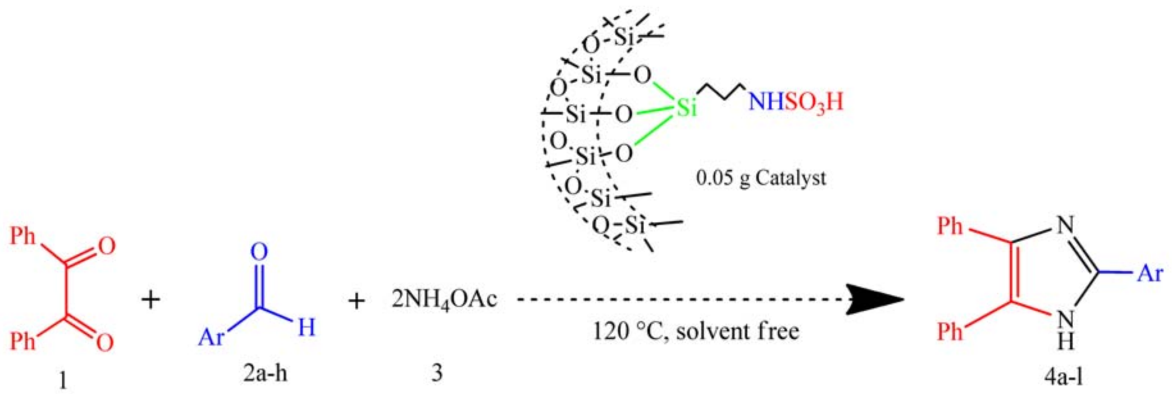

Fig. 4. Synthesis of 2,4,5-triaryl-1*H*-imidazoles using the NHSO$_3$H-KIT-5 catalyst.

Table 3. Optimized conditions for the synthesis of 2,4,5-triaryl-1*H*-imidazoles^a

Aldehyde	Product	Time min	Yield^b %	M.p./℃ experimental	 literature	Reference
Benzaldehyde	4a	10	90	273–275	274–276	Karimi et al. (2010)
3-NO_2-Benzaldehyde	4b	20	87	267–268	265–267	Karimi et al. (2010)
4-Cl-Benzaldehyde	4c	14	89	260–262	256–260	Karimi et al. (2010)
4-MeO-Benzaldehyde	4d	10	92	230–231	228–231	Karimi et al. (2010)
3-MeO-Benzaldehyde	4e	11	88	258–260	259–262	Heravi et al. (2007a)
4-Me-Benzaldehyde	4f	20	85	230–232	229–231	Heravi et al. (2007a)
2,4-diCl-Benzaldehyde	4g	18	83	174–175	174–175	Heravi et al. (2008b)
2-Cl-Benzaldehyde	4h	14	87	197–199	197–199	Heravi et al. (2007a)
4-NO_2-Benzaldehyde	4i	25	88	235–237	235–238	Heravi et al. (2007a)
4-Br-Benzaldehyde	4j	18	87	260–262	259	Heravi et al. (2007a)
4-$CH(CH_3)_2$-Benzaldehyde	4k	11	91	253–255	255–257	Bakavoli et al. (2015)
2-NO_2-Benzaldehyde	4l	20	83	228–230	230–231	Heravi et al. (2007a)

a) Reaction conditions: benzil (1.0 mmol), aromatic aldehyde (1.0 mmol), ammonium acetate (2.0 mmol), and NHSO$_3$H-KIT-5 as a catalyst (0.05 g), solvent-free at 120℃; *b*) yield refers to pure and isolated products.

compounds and found to be identical (Karimi et al., 2010; Heravi et al., 2007a, 2008b).

Spectral (IR and ^{13}C NMR) data for the model compound (2,4,5-triphenyl-1*H*-imidazole, 4a) are as follows: light-yellow solid, m.p. 273–275℃ (274–276℃ (Karimi et al., 2010)). $C_{21}H_{16}N_2$ composition, w_i/mass %: found C, 85.02; H, 5.1; N, 9.12; computed C, 85.11, H, 5.44, N, 9.45. IR (KBr), ν/cm^{-1}: 3435, 2993, 2471, 1638, 1215.

Results and discussion

Catalyst characterization

Samples were analyzed by FT-IR spectroscopy using a Perkin–Elmer 65, Islamic Azad University (Iran) in a KBr matrix in the range of 4000–400 cm^{-1}. X-ray diffraction (XRD) patterns of the materials were recorded on a Bruker D8 Advanced powder X-ray diffractometer, Esfahan University (Iran) using CuK_α (λ = 1.54 Å) radiation in the 2θ range of 2–80°. A scanning electron microscope (SEM) Lecia Cambridge S 360 (Cambridge, UK) was used to observe the morphology of the modified and unmodified mesoporous silica materials. Energy dispersive X-ray spectroscopy (EDXS) Genesis, Iran Polymer and Petrochemical Institute (Iran), with an SUTW detector equipped with SEM, was used to carry out the EDXS analysis in order to confirm the presence of silica. Thermal gravimetric analysis (TGA) data were obtained by a Setaram Labsys TG (STA), Islamic Azad University (Iran) in the temperature range of 10–700℃ and the heating rate of 5℃ min^{-1} under N_2 atmosphere.

Fig. 5 shows the wide-angle XRD pattern of the NH_2-KIT-5 (a) and NHSO$_3$H-KIT-5 catalyst (b). XRD patterns of the catalysts showed a decrease in the peak intensity due to the presence of a sulfur group inside the modified mesopores, leading to false diffraction. The reduced intensity revealed that organic moieties were present in the pores of NH_2-KIT-5. Moreover, this observation also confirmed the immobilization of SO_3H inside the mesopores of KIT-5 and the preparation of acid catalyst, NHSO$_3$H-KIT-5, which can be attributed to the symmetry being destroyed by

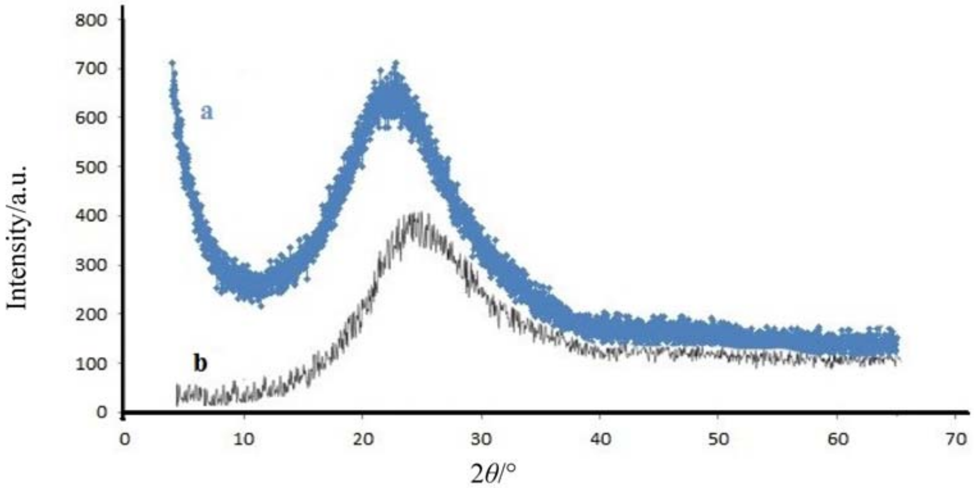

Fig. 5. WAXRD pattern of the NH_2-KIT-5 (a) and $NHSO_3H$-KIT-5 nanocatalyst (b).

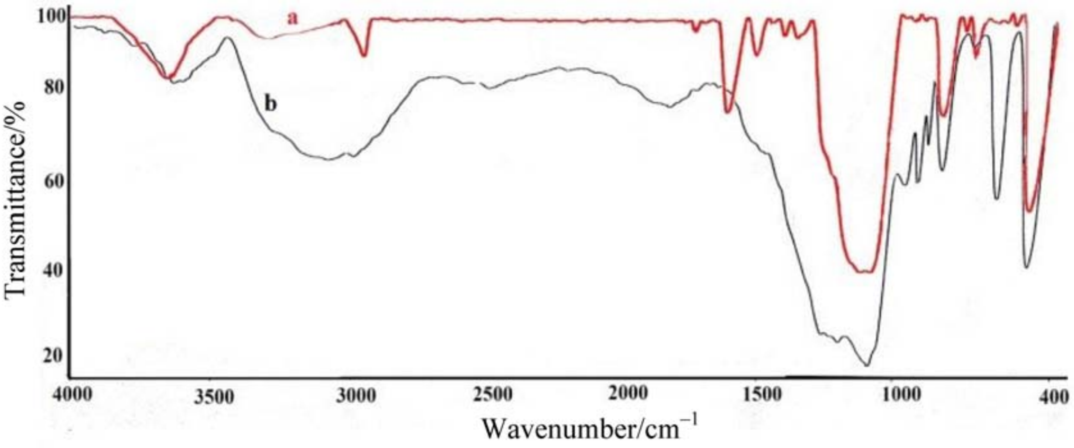

Fig. 6. FT-IR spectrum of the NH_2-KIT-5 (a) and $NHSO_3H$-KIT-5 catalyst (b).

the hybridization of ordered mesoporous silica loaded with guest matter.

Moreover, conversion of the amino group in NH_2-KIT-5 to $NHSO_3H$-KIT-5 was confirmed by FT-IR spectra. Fig. 6 shows the IR spectrum before and after the reaction of NH_2-KIT-5 with chlorosulfonic acid with the major peaks for silica including the broad anti-symmetric stretching Si—O—Si (1300–1000 cm^{-1}) and the symmetric stretching (820–740 cm^{-1}) were observed. In the NH_2-KIT-5 spectrum, the 2935 cm^{-1} peak can be assigned to the C—H bond stretching, while the NH_2 group showed two bands for primary amines, the N—H stretching (3390 cm^{-1}) and the N—H bending (1650 cm^{-1}). In comparison to the NH_2-KIT-5 sample, the distinguished features of N-SO_3H/KIT-5 were: the presence of a new absorption peak near 1032 cm^{-1} assigned to the symmetric stretching of the S═O bond as a result of the SO_3H groups in mesoporous silica, and an absorption band at 610 cm^{-1} due to the bending vibration of the OH groups hydrogen bonded to the SO_3H moieties. For the sulfamic acid functional group in the catalyst, the FT-IR spectrum showed overlapping asymmetric and symmetric stretching bands of the O═S═O with Si—O—Si stretching bands in the silica functionalized alkylsulfuric acid. The SO_2 asymmetric and symmetric stretching modes were positioned at 1170 cm^{-1} and 1060 cm^{-1}, respectively. The spectrum also showed a broad OH stretching absorption from 3600 cm^{-1} to 3200 cm^{-1}. NH stretching and bending signals appeared at 3420 cm^{-1} and 1650 cm^{-1}, respectively. In the catalyst spectrum, the (C—N) peak showed a slight positive shift, indicating that sulfur is chelated with nitrogen atoms onto NH_2-KIT-5. Therefore, the mesopore support can act as a chelate, which results in an increase of the amount of acid groups in the structure of the catalyst.

Morphology of the catalyst surface was analyzed by a SEM microscope equipped with an energy dispersive X-ray analyzer (EDXS). In a previous work, aminated KIT-5 and the following nanocopper synthesis on this nanosupport was presented (Mirsafaei

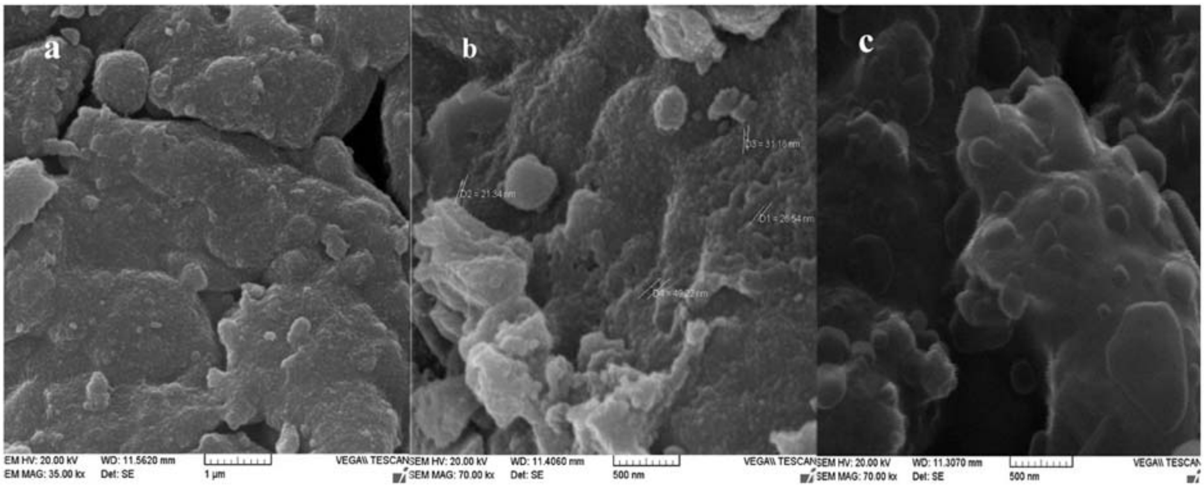

Fig. 7. SEM images of pure KIT-5 (a), modified KIT-5 (b), and the catalyst (c).

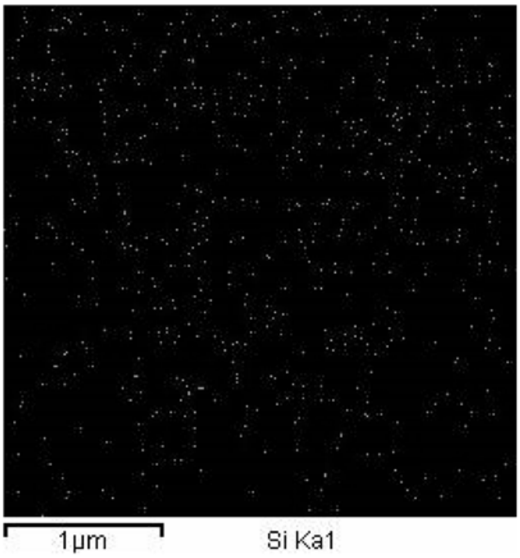

Fig. 8. Map image of the nanocatalyst.

et al. 2015). Fig. 7 shows the SEM images of pure KIT-5 (Fig. 7a), aminated KIT-5 (Fig. 7b), and the catalyst (Fig. 7c). Clear and vivid changes in the SEM micrographs were observed. The primary structure of pure KIT-5 was completely changed step by step (Figs. 7a–7c) after chemical modifications (Fig. 7b) and nanocatalyst addition (Fig. 7c), the aggregation of particles was prevented in the NHSO$_3$H-KIT-5 catalyst (Fig. 7c). Fig. 7c clearly demonstrates the changes in the morphology of the catalyst surface area that can be mainly attributed to the presence of sulfamic groups in the catalyst. Consequently, the surface area of the catalyst was covered uniformly retarding thus aggregation and increasing the catalytic activity in the organic transformations. The size of modified KIT-5 (Fig. 7b) was around 21–49 nm.

Due to the catalyst insolubility in all common organic solvents, only the SEM, EDAX, Map, and XRD analysis techniques could be used for structural elucidation. Fig. 8 shows a Map image of the nanocatalyst with the sulfur group homogeneously immobilized on the modified surface. The map of the catalyst approved this homogenous dispersion.

EDX data obtained for the catalyst also confirmed the addition of ClSO$_3$H on the surface of the modified KIT-5 matrix, suggesting thus the formation of an *N*-sulfamic acid linkage to the amine ligand via the anchored SO$_3$H group (Fig. 9).

Thermal stability of the NH$_2$-KIT-5 and *N*-sulfonamic acid catalyst was initially examined by the TGA analysis (under flowing of N$_2$), confirming the incorporation of SO$_3$H groups in NH$_2$-KIT-5. The two curves observed showed the mass loss of organic materials as they decomposed upon heating (Fig. 9). As illustrated in Fig. 10, NH$_2$-KIT-5 showed a slight loss of mass (about 5 %) below 150 ℃, probably due to the loss of a small quantity of adsorbed water. The observed mass loss course of *N*-sulfonamic acid below 150 ℃ was comparable to that of NH$_2$-KIT-5, where the mass loss occurred at about 350 ℃ caused probably by the decomposition of the aminopropyl group. Nevertheless, the TGA curve of *N*-sulfonamic acid at higher temperatures illustrated a more remarkable mass loss in comparison to that observed in NH$_2$-KIT-5. This can be chiefly attributed to the gradual desorption and thermal decomposition of the SO$_3$H group. It is expected that the *N*-sulfamic groups decompose at lower temperatures in comparison with APTES. The total percentage of the mass loss of the catalyst was estimated to be around 18 %, and 7 % in APTES/KIT-5. Such mass loss in the *N*-sulfonamic acid catalyst also proves the presence of *N*-sulfumic acid inside the pores. This catalyst is stable up to 220 ℃ and can be considered as a catalyst of choice in various organic reactions requiring the temperature range of 80–140 ℃ (Kleitz et al., 2003; Sharma et al.,

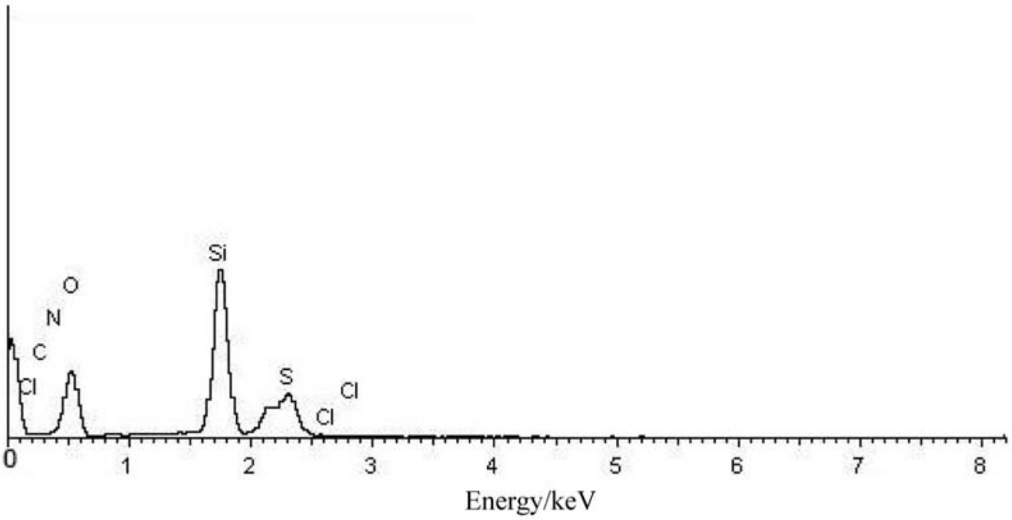

Fig. 9. EDXS analysis of the $NHSO_3H$-KIT-5 nanocatalys.

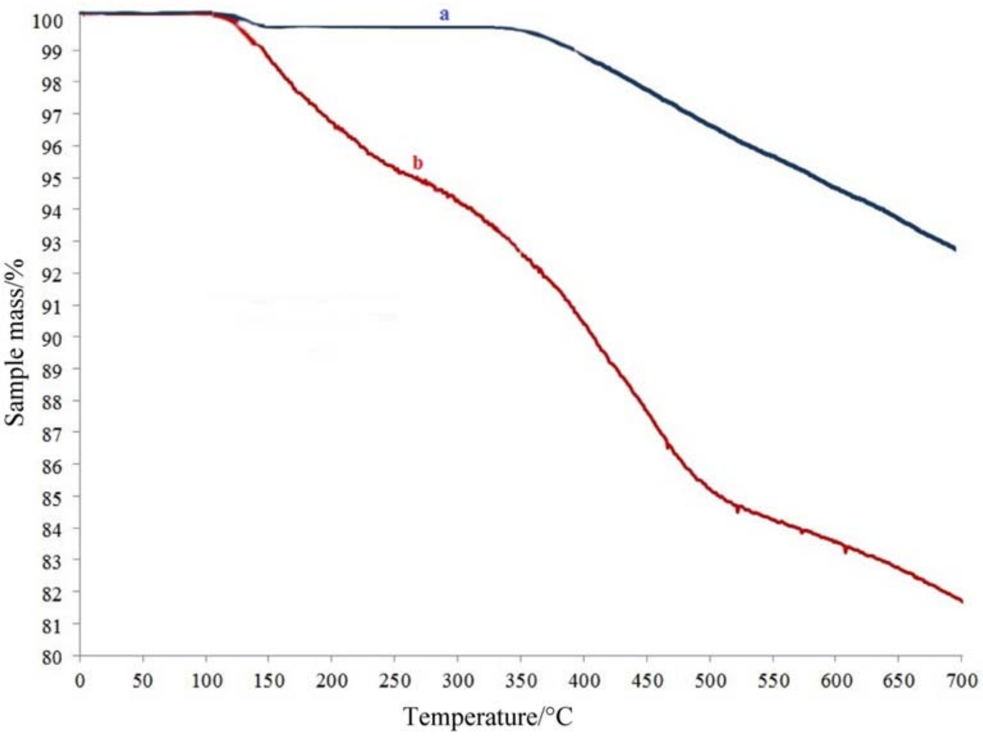

Fig. 10. TGA curve of the NH_2-KIT-5 (a) and $NHSO_3H$-KIT-5 catalyst (b).

2008). However, NH_2-KIT-5 is thermally stable even up to 400 ℃, therefore it is frequently employed as a thermally stable catalyst support in several organic transformations.

Preparation and characterization of 2,4,5-triaryl-1H-imidazoles

In order to investigate, the catalytic activity of the prepared $NHSO_3H$-KIT-5 nanocatalyst, the synthesis of trisubstituted imidazoles was performed; results are given in Table 2. A mixture of various aldehydes (1 mmol), benzil (1 mmol), ammonium acetate (2 mmol), and $NHSO_3H$-KIT-5 (0.05 g) as the nanocatalyst were reacted under solvent-free conditions. To find the optimal reaction conditions, the synthesis of 4a was selected as a model reaction. This reaction was performed in different solvents such as H_2O, CH_3CH_2OH, and CH_3CN. Interestingly, the solvent-free system gave the best results in terms of yield and reaction time (Table 4). As it can be seen, different solvents (H_2O, CH_3CH_2OH, and CH_3CN)

Table 4. Optimization of conditions for the synthesis of 4a in the presence of the $NHSO_3H$-KIT-5 catalyst^a

Entry	Solvent and conditions	Catalyst (g)	Time (min)	Yield^b (%)
1	H_2O, reflux	0.05	30	63
2	EtOH, reflux	0.05	35	58
3	CH_3CN, reflux	0.05	43	59
4	Solvent-free, 100 ℃	0.06	17	75
5	Solvent-free, 100 ℃	0.05	17	75
6	Solvent-free, 100 ℃	0.04	20	70
7	Solvent-free, 100 ℃	0.03	30	70
8	Solvent-free, 110 ℃	0.05	16	80
9	Solvent-free, 120 ℃	0.05	10	90
10	Solvent-free, 130 ℃	0.05	16	90

a) Reaction conditions: benzaldehyde (1 mmol), benzil (1 mmol), ammonium acetate (2 mmol) in 2 mL of solvent (in solution experiment); *b*) yield refers to isolated and pure product.

Table 5. Comparison of the efficiency of various catalysts with $NHSO_3H$-KIT-5 in the synthesis of 2,4,5-trisubstituted imidazoles

Entry	Catalyst	Conditions	Time min	Yield^a %	Reference
1	KH_2PO_4	EtOH/Reflux	60	89	Heravi and Alishiri (2012)
2	$InCl_3 \cdot 3H_2O$	MeOH/R.T	492	76	Heravi et al. (2010)
3	$Zr(acac)_4$	EtOH/Reflux	120	95	Khosropour (2008)
4	L-proline	MeOH/60 ℃	540	87	Samai et al. (2009)
5	$NiCl_2 \cdot 6H_2O/Al_2O_3$	EtOH/Reflux	90	89	Heravi et al. (2009a)
6	(4-SB)T (4-SPh) $PHSO_4$ (15 mole %)	Solvent-free /120 ℃	15	94	Heravi et al. (2009b)
7	$NHSO_3H$-KIT-5 (0.05 g)	Solvent-free /120 ℃	10	90	This study

a) Yield refers to isolated and pure product.

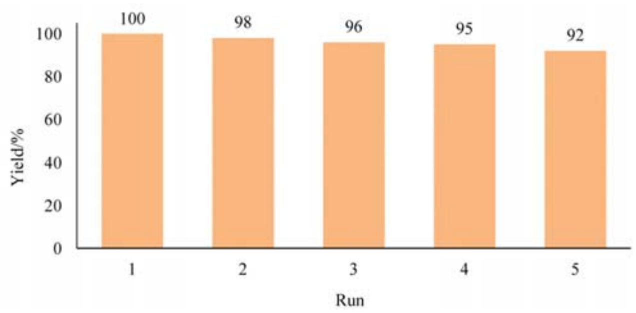

Fig. 11. Recyclability of the $NHSO_3H$-KIT-5 nanocatalyst in the preparation of 4a.

were compared with the reaction in solvent-free conditions at different temperatures and with various amounts of the catalyst. According to the results, solvent-free conditions were chosen which is dictated by the green chemistry principles. Optimization of the amount of the catalyst was also studied. As shown in Table 4, entry 9, the best result was achieved in the presence of 0.05 g of $NHSO_3H$-KIT-5 at 120 ℃ in solvent free conditions.

To show the advantages of $NHSO_3H$-KIT-5 as a heterogeneous acid nanocatalyst, the reaction conditions of the synthesis of 2,4,5-triphenyl-1*H*-imidazole (4a) were compared with those using various catalysts, reported previously (Table 5). The results showed that the catalyst performance of the presented nanocatalyst is quite comparable with those of the already reported ones, regarding the yields and reaction times.

Reusability of the catalyst was also tested (Fig. 11); the model reaction (synthesis of 4a) was conducted five times with recycled catalysts under similar conditions and only non-appreciable mass loss was observed in the obtained desired compound. After each cycle, the catalyst was filtered off, washed with water (10 mL), dried in an oven at 70 ℃ and reused in the next reaction cycle without any further modification.

Conclusions

In conclusion, a mild, recoverable and efficient heterogeneous catalyst was prepared and employed for the catalysis of a one-pot multicomponent biologically important reaction. In the aforementioned reaction, trisubstituted imidazoles were produced from benzil, aromatic aldehydes, and ammonium acetate in the presence of 0.05 g of the catalyst under solvent-free conditions. A simple and efficient catalyst has been prepared using a silica type mesoporous material, KIT-5, which is the best choice as a support due to its maximum surface area (1090 $m^2\ g^{-1}$). As shown in Table 1, the catalyst has a large surface area and highly ordered mesoporous nanocage structure with cubic Fm3m close packed symmetric ordering, large pores, and high specific pore volume (Kleitz et al., 2003). The XRD and SEM results showed the hybrid character of KIT-5 supported on APTES as an organic–inorganic hybrid catalyst. Moreover, based on DFT computed results, immobilization of SO_3H inside the mesopores of KIT-5 was confirmed. In this respect, the sulfur atom was proved to be chelated with a nitrogen atom on NH_2-KIT-5 rather than on an oxygen atom confirming the effective preparation of acid catalyst on N-SO_3H/KIT-5. Therefore, in order to activate the catalyst surface, an appropriate moiety should be linked to it. On the other hand, this hybrid catalyst has better properties than SiO_2. The prepared heterogeneous catalyst was found stable at high temperatures, highly active, and recyclable, which is desired for catalyzed imidazole reactions in high yields, providing shorter reaction time than the previously described catalysts. It is worthwhile to mention that this catalyzed reaction is facile, clean, and no tedious work-up procedure or separation techniques are required. Therefore, the highly mesoporous silica KIT-5 catalyst should be considered and studied as a smart support for other nanocatalysts used in various catalyzed organic reactions. The ease of separation along with its recyclability are the other advantages of this mesoporous nanocatalyst.

Acknowledgements. Professor Heravi is grateful for partial financial support from the Iran National Science Foundation. The authors are thankful to the Iran Polymer and Petrochemical Institute for providing the SEM-EDXS facility, the Kashan University for providing XRD analysis and the Islamic Azad Yazd University for providing IR analysis.

References

Bader, R. F. W., & Essén, H. (1984). The characterization of atomic interactions. *The Journal of Chemical Physics*, *80*, 1943–1960. DOI: 10.1063/1.446956.

Bader, R. F. W. (1990). *Atoms in molecules: A quantum theory.* Oxford, UK: Oxford University Press.

Bader, R. F. W. (2000). AIM2000 program, ver. 2.0 [computer software]. Hamilton, Canada: McMaster University.

Bakavoli, M., Eshghi, H., Rahimizadeh, M., Housaindokht, M. R., Mohammadi, A., & Monhemi, H. (2015). Deep eutectic solvent for multi-component reactions: a highly efficient and reusable acidic catalyst for synthesis of 2,4,5-triaryl-1H-imidazoles. *Research on Chemical Intermediates*, *41*, 3497–3505. DOI: 10.1007/s11164-013-1467-7.

Bamoharram, F. F., Heravi, M. M., Roshani, M., Jahanagir, M., & Gharib, A. (2007). Effective direct esterification of butanol by eco-friendly Preyssler catalyst, $[NaP_5W_{30}O_{110}]^{14-}$. *Journal of Molecular Catalysis A: Chemical*, *271*, 126–130. DOI: 10.1016/j.molcata.2007.02.034.

Blotny, G. (2006). Recent applications of 2,4,6-trichloro-1,3,5-triazine and its derivatives in organic synthesis. *Tetrahedron*, *62*, 9507–9522. DOI: 10.1016/j.tet.2006.07.039.

Davoodnia, A., Heravi, M. M., Safavi-Rad, Z., & Tavakoli-Hoseini, N. (2010). Green, one-pot, solvent-free synthesis of 1,2,4,5-tetrasubstituted imidazoles using a Brønsted acidic ionic liquid as novel and reusable catalyst. *Synthetic Communications*, *40*, 2588–2597. DOI: 10.1080/00397910903289271.

Fan, X. S., Qu, Y. Y., Wang, Y. Y., Zhang, X. Y., & Wang, J. J. (2010). Ru(III)-catalyzed oxidation of homopropargyl alcohols in ionic liquid: an efficient and green route to 1,2-allenic ketones. *Tetrahedron Letters*, *51*, 2123–2126. DOI: 10.1016/j.tetlet.2010.02.053.

Guisnet, M., Barrault, J., Bouchoule, C., Duprez, D., Montassier, C., & Pérot, G. (Eds.) (1988). *Heterogeneous catalysis and fine chemicals* (Studies in surface science, Vol. *41*). Amsterdam, The Netherlands: Elsevier.

Hamon, F., Prié, G., Lecornué, F., & Papot, S. (2009). Cyanuric chloride: an efficient reagent for the Lossen rearrangement. *Tetrahedron Letter*, *50*, 6800–6802. DOI: 10.1016/j.tetlet.2009.09.115.

Hashemi, E., Beheshtiha, Y. S., Ahmadi, S., & Heravi, M. M. (2014). In situ prepared CuI nanoparticles on modified poly(styrene-co-maleic anhydride): an efficient and recyclable catalyst for the azide–alkyne click reaction in water. *Transition Metal Chemistry*, *39*, 593–601. DOI: 10.1007/s11243-014-9838-5.

Heravi, M. M., Montazeri, N., Rahmizadeh, M., Bakavoli, M., & Ghassemzadeh, M. (2000). Zeolite-induced heterocyclization: a superior method of synthesis of condensed imidazoles. *Journal of Chemical Research*, *2000*, 584–585. DOI: 10.3184/030823400103166274.

Heravi, M. M., Rajabzadeh, G., Bamoharram, F. F., & Seifi, N. (2006a). An eco-friendly catalytic route for synthesis of 4-amino-pyrazolo[3,4-d]pyrimidine derivatives by Keggin heteropolyacids under classical heating and microwave irradiation. *Journal of Molecular Catalysis A: Chemical*, *256*, 238–241. DOI: 10.1016/j.molcata.2006.04.016.

Heravi, M. M., Tajbakhsh, M., Ahmadi, A. N., & Mohajerani, B. (2006b). Zeolites. Efficient and eco-friendly catalysts for the synthesis of benzimidazoles. *Monatshefte für Chemie - Chemical Monthly*, *137*, 175–179. DOI: 10.1007/s00706-005-0407-7.

Heravi, M. M., Bakhtiari, K., Oskooie, H. A., & Taheri, S. (2007a). Synthesis of 2,4,5-triaryl-imidazoles catalyzed by $NiCl_2·6H_2O$ under heterogeneous system. *Journal of Molecular Catalysis A: Chemical*, *263*, 279–281. DOI: 10.1016/j.molcata.2006.08.070.

Heravi, M. M., Bakhtiari, K., Daroogheha, Z., & Bamoharram, F. F. (2007b). An efficient synthesis of 2,4,6-triarylpyridines catalyzed by heteropolyacid under solvent-free conditions. *Catalysis Communications*, *8*, 1991–1994. DOI: 10.1016/j.catcom.2007.03.028.

Heravi, M. M., Bakhtiari, K., Zadsirjan, V., Bamoharram, F. F., & Heravi, O. M. (2007c). Aqua mediated synthesis of substituted 2-amino-4H-chromenes catalyzed by green and reusable Preyssler heteropolyacid. *Bioorganic & Medicinal Chemistry Letters*, *17*, 4262–4265. DOI: 10.1016/j.bmcl.2007.05.023.

Heravi, M. M., Derikvand, F., & Bamoharram, F. F. (2007d). Highly efficient, four-component one-pot synthesis of tetrasubstituted imidazoles using Keggin-type heteropolyacids as green and reusable catalysts. *Journal of Molecular Catalysis A: Chemical*, *263*, 112–114. DOI: 10.1016/j.molcata.2006.08.048.

Heravi, M. M., Bakhtiari, K., Fatehi, A., & Bamoharram, F. F. (2008a). A convenient synthesis of bis(indolyl)methanes catalyzed by diphosphooctadecatungstic acid. *Catalysis Communications*, *9*, 289–292. DOI: 10.1016/j.catcom.2007.07.039.

Heravi, M. M., Derikvand, F., & Haghighi, M. (2008b). Highly efficient, four component, one-pot synthesis of tetrasubstituted imidazoles using a catalytic amount of $FeCl_3 \cdot 6H_2O$. *Monatshefte für Chemie - Chemical Monthly*, *139*, 31–33. DOI: 10.1007/s00706-007-0736-9.

Heravi, M. M., & Sadjadi, S. (2009). Recent developments in use of heteropolyacids, their salts and polyoxometalates in organic synthesis. *Journal of the Iranian Chemical Society*, *6*, 1–54. DOI: 10.1007/bf03246501.

Heravi, M. M., Sadjadi, S., Sadjadi, S., Oskooie, H. A., & Bamoharram, F. F. (2009a). Rapid and efficient synthesis of 4(3*H*)-quinazolinones under ultra sonic irradiation using silica-supported Preyssler nano particles. *Ultrasonics Sonochemistry*, *16*, 708–710. DOI: 10.1016/j.ultsonch.2009.02.010.

Heravi, M. M., Sadjadi, S., Sadjadi, S., Oskooie, H. A., & Bamoharram, F. F. (2009b). A convenient synthesis of bis(indolyl)alkanes under ultra sonic irradiation using silica-supported Preyssler nano particles. *Ultrasonics Sonochemistry, 16*, 718–720. DOI: 10.1016/j.ultsonch.2009.04.004.

Heravi, M. M., Tavakoli-Hoseini, N., & Bamoharram, F. F. (2010). Silica-supported Preyssler nano particles: a green, reusable and highly efficient heterogeneous catalyst for the synthesis of carbamatoalkyl naphthols. *Green Chemistry Letters and Reviews*, *3*, 263–267. DOI: 10.1080/17518251003749387.

Heravi, M. M., & Alishiri, T. (2012). Application of nanomaterials in heterocyclic chemistry. *Heterocycles*, *85*, 545–586. DOI: 10.3987/rev-11-725.

Heravi, M. M., Hashemi, E., Beheshtiha, Y. S., Ahmadi, S., & Hosseinnejad, T. (2014). $PdCl_2$ on modified poly(styrene-co-maleic anhydride): A highly active and recyclable catalyst for the Suzuki–Miyaura and Sonogashira reactions. *Journal of Molecular Catalysis A: Chemical*, *394*, 74–82. DOI: 10.1016/j.molcata.2014.07.001.

Heravi, M. M., Daraie, M., & Zadsirjan, V. (2015). Current advances in the synthesis and biological potencies of *tri*- and *tetra*-substituted *1H*-imidazoles. *Molecular Diversity*, *19*, 577–623. DOI: 10.1007/s11030-015-9590-6.

Karimi, A. R., Alimohammadi, Z., & Amini, M. M. (2010). Wells–Dawson heteropolyacid supported on silica: a highly efficient catalyst for synthesis of 2,4,5-trisubstituted and 1,2,4,5-tetrasubstituted imidazoles. *Molecular Diversity*, *14*, 635–641. DOI: 10.1007/s11030-009-9197-x.

Khorami, F., & Shaterian, H. R. (2014). Silica-bonded propylpiperazine-*N*-sulfamic acid as recyclable solid acid catalyst for preparation of 2-amino-3-cyano-4-aryl-5,10-dioxo-5,10-dihydro-4*H*-benzo[*g*]chromenes and hydroxy-substituted naphthalene-1,4-dione derivatives. *Chinese Journal of Catalysis*, *35*, 242–246. DOI: 10.1016/s1872-2067(12)60761-x.

Khosropour, A. R. (2008). Ultrasound-promoted greener synthesis of 2,4,5-trisubstituted imidazoles catalyzed by $Zr(acac)_4$ under ambient conditions. *Ultrasonics Sonochemistry*, *15*, 659–664. DOI: 10.1016/j.ultsonch.2007.12.005.

Kidwai, M., Mothsra, P., Bansal, V., Somvanshi, R. K., Ethayathulla, A. S., Dey, S., & Singh, T. P. (2007). One-pot synthesis of highly substituted imidazoles using molecular iodine: A versatile catalyst. *Journal of Molecular Catalysis A: Chemical*, *265*, 177–182. DOI: 10.1016/j.molcata.2006.10.009.

Kleitz, F., Liu, D. N., Anilkumar, G. M., Park, I. S., Solovyov, L. A., Shmakov, A. N., & Ryoo, R. (2003). Large cage face-centered-cubic $Fm3m$ mesoporous silica: Synthesis and structure. *The Journal of Physical Chemistry B*, *107*, 14296–14300. DOI: 10.1021/jp036136b.

Lee, C. T., Yang, W. T., & Parr, R. G. (1988). Development of the Colle-Salvetti correlation-energy formula into a functional of the electron density. *Physical Review B*, *37*, 785–789. DOI: 10.1103/PhysRevB.37.785.

Li, B. Z., Gu, Q., He, Y. H., Zhao, T. Q., Wang, S. J., Kang, J., & Zhang, Y. M. (2012). Facile synthesis of trisubstituted imidazoles from 1,2-di(furan-2-yl)-2-oxoethyl carboxylates and their chemiluminescence. *Comptes Rendus Chimie*, *15*, 784–792. DOI: 10.1016/j.crci.2012.06.005.

Liu, L., Ma, J. J., Ji, L. Y., & Wei, Y. Y. (2008). Molecular sieve promoted copper catalyzed aerobic oxidation of alcohols to corresponding aldehydes or ketones. *Journal of Molecular Catalysis A: Chemical*, *291*, 1–4. DOI: 10.1016/j.molcata.2008.06.001.

Mahdavinia, G. H., Amani, A. M., & Sepehrian, H. (2012). MCM-41-SO_3H as a highly efficient sulfonic acid nanoreactor for the rapid and green synthesis of some novel highly substituted imidazoles under solvent-free condition. *Chinese Journal of Chemistry*, *30*, 703–708. DOI: 10.1002/cjoc.201280008.

Mannam, S., & Sekar, G. (2008). CuCl catalyzed oxidation of aldehydes to carboxylic acids with aqueous *tert*-butyl hydroperoxide under mild conditions. *Tetrahedron Letters*, *49*, 1083–1086. DOI: 10.1016/j.tetlet.2007.11.198.

Martín, S. E., & Garrone, A. (2003). Efficient solvent-free iron(III) catalyzed oxidation of alcohols by hydrogen peroxide. *Tetrahedron Letters*, *44*, 549–552. DOI: 10.1016/s0040-4039(02)02569-8.

Mirsafaei, R., Heravi, M. M., Ahmadi, S., Moslemin, M. H., & Hosseinnejad, T. (2015). In situ prepared copper nanoparticles on modified KIT-5 as an efficient recyclable catalyst and its applications in click reactions in water. *Journal of Molecular Catalysis A: Chemical*, *402*, 100–108. DOI: 10.1016/j.molcata.2015.03.006.

Moghaddas, M., Davoodnia, A., Heravi, M. M., & Tavakoli-Hoseini, N. (2012). Sulfonated carbon catalyzed Biginelli reaction for one-pot synthesis of 3,4-dihydropyrimidin-2(1*H*)-ones and -thiones. *Chinese Journal of Catalysis*, *33*, 706–710. DOI: 10.1016/s1872-2067(11)60377-x.

Mohammadi, A. A., Mivechi, M., & Kefayati, H. (2008). Potassium aluminum sulfate (alum): an efficient catalyst for the one-pot synthesis of trisubstituted imidazoles. *Monatshefte für Chemie - Chemical Monthly*, *139*, 935–937. DOI: 10.1007/s00706-008-0875-7.

Mohammed, A. F., Kokare, N. D., Sangshetti, J. N., & Shinde, D. B. (2007). Sulphanilic acid catalyzed facile one-pot synthesis of 2,4,5-triarylimidazoles from benzil/benzoin and aromatic aldehydes. *Journal of the Korean Chemical Society*, *51*, 418–422. DOI: 10.5012/jkcs.2007.51.5.418.

Nemati, F., Heravi, M. M., & Saeedi Rad, R. (2012). Nano-Fe_3O_4 encapsulated-silica particles bearing sulfonic acid groups as a magnetically separable catalyst for highly efficient Knoevenagel condensation and Michael addition reactions of aromatic aldehydes with 1,3-cyclic diketones. *Chinese Journal of Catalysis*, *33*, 1825–1831. DOI: 10.1016/s1872-2067(11)60455-5.

Nouri Sefat, M., Deris, A., & Niknam, K. (2011). Preparation of silica-bonded propyl-diethylene-triamine-*N*-sulfamic acid as a recyclable catalyst for chemoselective synthesis of 1,1-diacetates. *Chinese Journal of Chemistry*, *29*, 2361–2367. DOI: 10.1002/cjoc.201180403.

Oskooie, H. A., Alimohammadi, Z., & Heravi, M. M. (2006a). Microwave-assisted solid-phase synthesis of 2,4,5-triaryl imidazoles in solventless system: An improved protocol. *Heteroatom Chemistry, 17*, 699–702. DOI: 10.1002/hc.20237.

Oskooie, H. A., Heravi, M. M., Bakhtiari, K., Zadsirjan, V., & Bamoharram, F. F. (2006b). $H_{14}[NaP_5W_{30}O_{110}]$ as an efficient catalyst for the one-pot synthesis of α-amino nitriles. *Synlett*, *2006*, 1768–1770. DOI: 10.1055/s-2006-944206.

Sadeghi, B., Mirjalili, B. B. F., & Hashemi, M. M. (2008). $BF_3 \cdot SiO_2$: an efficient reagent system for the one-pot synthesis of 1,2,4,5-tetrasubstituted imidazoles. *Tetrahedron Letters*, *49*, 2575–2577. DOI: 10.1016/j.tetlet.2008.02.100.

Samai, S., Nandi, G. C., Singh, P., & Singh, M. S. (2009). L-Proline: an efficient catalyst for the one-pot synthesis of 2,4,5-trisubstituted and 1,2,4,5-tetrasubstituted imidazoles. *Tetrahedron*, *65*, 10155–10161. DOI: 10.1016/j.tet.2009.10.019.

Sarshar, S., Siev, D., & Mjalli, A. M. M. (1996). Imidazole libraries on solid support. *Tetrahedron Letters*, *37*, 835–838. DOI: 10.1016/0040-4039(95)02334-8.

Schaubroeck, D., De Baets, J., Desmet, T., Van Vlierberghe, S., Schacht, E., & Van Calster, A. (2009). Introduction of amino groups on the surface of thin photo definable epoxy resin layers via chemical modification. *Applied Surface Science*, *255*, 8780–8787. DOI: 10.1016/j.apsusc.2009.06.043.

Schaubroeck, D., De Baets, J., Desmet, T., Dubruel, P., Schacht, E., Van Vaeck, L., & Van Calster, A. (2010). Surface modification of an epoxy resin with polyamines via cyanuric chloride coupling. *Applied Surface Science*, *256*, 6269–6278. DOI: 10.1016/j.apsusc.2010.04.003.

Schmidt, M. W., Baldridge, K. K., Boatz, J. A., Elbert, S. T., Gordon, M. S., Jensen, J. H., Koseki, S., Matsunaga, N., Nguyen, K. A., Su, S. J., Windus, T. L., Dupuis, M., & Montgomery, J. A., Jr. (1993). General atomic and molecular electronic structure system. *Journal of Computational Chemistry*, *14*, 1347–1363. DOI: 10.1002/jcc.540141112.

Shaabani, A., & Rahmati, A. (2006). Silica sulfuric acid as an efficient and recoverable catalyst for the synthesis of trisubstituted imidazoles. *Journal of Molecular Catalysis A: Chemical*, *249*, 246–248. DOI: 10.1016/j.molcata.2006.01.006.

Sharma, S. D., Hazarika, P., & Konwar, D. (2008). An efficient and one-pot synthesis of 2,4,5-trisubstituted and 1,2,4,5-tetrasubstituted imidazoles catalyzed by $InCl_3 \cdot 3H_2O$. *Tetrahedron Letters*, *49*, 2216–2220. DOI: 10.1016/j.tetlet.2008.02.053.

Sharma, R. K., & Sharma, C. (2011). Zirconium(IV)-modified silica gel: Preparation, characterization and catalytic activity in the synthesis of some biologically important molecules. *Catalysis Communications*, *12*, 327–331. DOI: 10.1016/j.catcom.2010.10.011.

Shvo, Y., & Goldman-Lev, V. (2002). Catalytic oxidation of alcohols with allyl diethyl phosphate and palladium acetate. *Journal of Organometallic Chemistry*, *650*, 151–156. DOI: 10.1016/s0022-328x(02)01177-4.

Siddiqui, S. A., Narkhede, U. C., Palimkar, S. S., Daniel, T., Lahoti, R. J., & Srinivasan, K. V. (2005). Room temperature ionic liquid promoted improved and rapid synthesis of 2,4,5-triaryl imidazoles from aryl aldehydes and 1,2-diketones or α-hydroxyketone. *Tetrahedron*, *61*, 3539–3546. DOI: 10.1016/j.tet.2005.01.116.

Silva, A. R., Freire, C., de Castro, B., Freitas, M. M. A., & Figueiredo, J. L. (2001). Anchoring of a nickel(II) Schiff base complex onto activated carbon mediated by cyanuric chloride. *Microporous and Mesoporous Materials*, *46*, 211–221. DOI: 10.1016/s1387-1811(01)00297-9.

Silva, A. R., Wilson, K., Clark, J. H., & Freire, C. (2006). Covalent attachment of chiral manganese(III) *salen* complexes onto functionalised hexagonal mesoporous silica and application to the asymmetric epoxidation of alkenes. *Microporous and Mesoporous Materials*, *91*, 128–138. DOI: 10.1016/j.micromeso.2005.11.032.

Silva, A. R., Budarin, V., Clark, J. H., Freire, C., & de Castro, B. (2007). Organo-functionalized activated carbons as supports for the covalent attachment of a chiral manganese(III) *salen* complex. *Carbon*, *45*, 1951–1964. DOI: 10.1016/j.carbon.2007.06.013.

Suib, S. L. (2013). *New and future developments in catalysis*. Amsterdam, The Netherlands: Elsevier. DOI: 10.1016/b978-0-444-53874-1.00022-6.

Tao, F., Nguyen, L., & Zhang, S. (2014). Introduction: Synthesis and catalysis on metal nanoparticles. In F. Tao (Ed.), *Metal nanoparticles for catalysis: Advances and applications* (RSC Catalysis Series, pp. 1–5). Cambridge, UK: The Royal Society of Chemistry. DOI: 10.1039/9781782621034-00001.

Wang, X. B., He, L., Jian, T. Y., & Ye, S. (2012). Cyclic phosphoric acid catalyzed one-pot, four-component synthesis of 1,2,4,5-tetrasubstituted imidazoles. *Chinese Chemical Letters*, *23*, 13–16. DOI: 10.1016/j.cclet.2011.09.018.

Zeinali-Dastmalbaf, M., Davoodnia, A., Heravi, M. M., Tavakoli-Hoseini, N., Khojastehnezhad, A., & Zamani, H. A. (2011). Silica gel-supported polyphosphoric acid (PPA-SiO_2) catalyzed one-pot multi-component synthesis of 3,4-dihydropyrimidin-2(1*H*)-ones and -thiones: An efficient method for the Biginelli reaction. *Bulletin of Korean Chemical Society*, *32*, 656–658. DOI: 10.5012/bkcs.2011.32.2.656.

Zhao, Y., & Truhlar, D. G. (2008). The M06 suite of density functionals for main group thermochemistry, thermochemical kinetics, noncovalent interactions, excited states, and transition elements: two new functionals and systematic testing of four M06-class functionals and 12 other functionals. *Theoretical Chemistry Accounts*, *120*, 215–241. DOI: 10.1007/s00214-007-0310-x.

Zhao, X. N., Hu, H. C., Zhang, F. J., & Zhang, Z. H. (2014). Magnetic $CoFe_2O_4$ nanoparticle immobilized *N*-propyl diethylenetriamine sulfamic acid as an efficient and recyclable catalyst for the synthesis of amides via the Ritter reaction. *Applied Catalysis A: General*, *482*, 258–265. DOI: 10.1016/j.apcata.2014.06.006.